Magnetic Resonance Image Enhancement by Reducing Receptors' Effective Size and Enabling Multiple Channel Acquisition

Fernando Yepes-Calderon[1,4], Adriana Velasquez[1], Natasha Lepore[3,4] and Olivier Beuf[2]

***Abstract*— Magnetic resonance imaging is empowered by parallel reading, which reduces acquisition time dramatically. The time saved by parallelization can be used to increase image quality or to enable specialized scanning protocols in clinical and research environments. In small animals, the sizing constraints render the use of multi-channeled approaches even more necessary, as they help to improve the typically low spatial resolution and lesser signal-to-noise ratio; however, the use of multiple channels also generates mutual induction (MI) effects that impairs imaging creation. Here, we created coils and used the shared capacitor technique to diminish first degree MI effects and pre-amplifiers to deal with higher order MI-related image deterioration. The constructed devices are tested by imaging phantoms that contain identical solutions; thus, creating the conditions for several statistical comparisons. We confirm that the shared capacitor strategy can recover the receptor capacity in compounded coils when working at the dimensions imposed by small animal imaging. Additionally, we demonstrate that the use of pre-amplifiers does not significantly reduce the quality of the images. Moreover, in light of our results, the two MI-avoiding techniques can be used together, therefore establishing the practical feasibility of flexible array coils populated with multiple loops for small animal imaging.**

I. INTRODUCTION

Magnetic Resonance Imaging (MRI) has become an ubiquitous tool in imaging research and clinical radiology due to its capacity to provide non-invasive, in-vivo images, both in humans and animal models. Small animals are widely used in disease research as their size make them particularly easy to manipulate; however, MR imaging is also significantly more challenging in smaller structures. The trade-off between the spatial resolution and signal-to-noise ratio (SNR) becomes exceptionally important when scanning small volumes.

Despite improvements in high field magnet technology at 7T and beyond, several factors reduce image quality so that higher fields may not mean better images [2]. In contrast, parallel acquisitions improve image quality no matter the magnet power [12]. Simultaneous acquisitions require single receptors to be split into two or more elementary coils while maintaining the field of view (FOV). This dimensional reduction is, initially, convenient on the grounds that smaller receptors provide higher sensitivity and field stability [12], [5]. Nevertheless, when two or more coils share a common space, their mutual inductance (MI) [13] deteriorates the receptor characteristics of the coils to the point where images cannot be produced.

[1]Universidad de Barcelona, C. de casanova 143, Barcelona-Spain.
[2]Université de Lyon, CREATIS; INSA-Lyon, Villeurbanne, France.
[3]University of Southern California, 900 W 34th St, LA CA-USA.
[4]Children Hospital Los Angeles, 4650 Sunset Blvd, LA CA-USA.

Here, we present strategies to increase the quality of MRI images acquired with arrays of surface coils by minimizing the deteriorating effects of MI. The first strategy involves a shared capacitor placed between adjacent loops that counteracts the rising MI at Larmor frequency (F_r) [8]. A second strategy, accomplished with pre-amplifiers, consists in diminishing the electrons' flow among the receptors, so the factor $L\frac{di}{dt}$ is smaller; therefore, MI is diminished as well [11]. This last strategy is intended to deal with high order MI, which is likely to be an issue when reading parallelization involves more than two channels. We also determine the effect of implementing these MI reducing strategies both independently and combined by analyzing the SNR, the field stability and the sensitivity of the coils for the images produced.

II. MATERIALS AND METHODS

All experiments presented here were performed using a Biospec 4.7T MRI Bruker system, configured to enable the surface coil mode and parallel imaging. Homemade printed card board (PCB) surface coils designed using the Eagle software [4] were placed as receptors. The loops' circuitry was created following the procedure depicted in [1]. The devices were simulated and tested individually in a network analyzer (Agilent - E5062A-275) before coupling them to the MRI scanner. All coils were matched at 50Ω and tuned at Larmor frequency (f_r) which corresponds to 200.3 MHz, as dictated by hydrogen spins magnetized at 4.7T.

The created devices consist of: A single-loop receptor (**SD**), a two-loops receptor with shared capacitor (**DD**), a single-loop receptor with low impedance amplifier (**SDWP**) and a two-loops receptor with shared capacitor and pre-amplifiers (**DDWP**). All the loops used to create the devices listed above have $15mm$ in diameter. **Fig. 1** shows the testing receptors.

With the surface coils placed into the scanner, images were acquired on phantoms using T1 contrast and multi-slice-multi-echo sequence (MSME-pvm) [7]. The parameters of these images are: repetition and echo times (TR and TE) of 261.4 and 10.7 ms respectively, with a flip angle of $180°$; isometric in-plane resolution of $0.136mm$; slice thickness of $2mm$; $35x35mm^2$ FOV; $256x256$ matrix, 8 slices for single loop coils, and 16 for the two-elements ones. Acquisition time is kept at 3.06 minutes for all experiments. The phantom for single loops coils consists of a circular syringe $15mm$ in diameter, while the two-elements devices scanned a syringe of $30mm$ in diameter. Both phantoms contain a mix of water, salt (4.5%) and gadolinium. We perform six acquisitions

978-1-4244-7929-0/14/$26.00 ©2014 IEEE

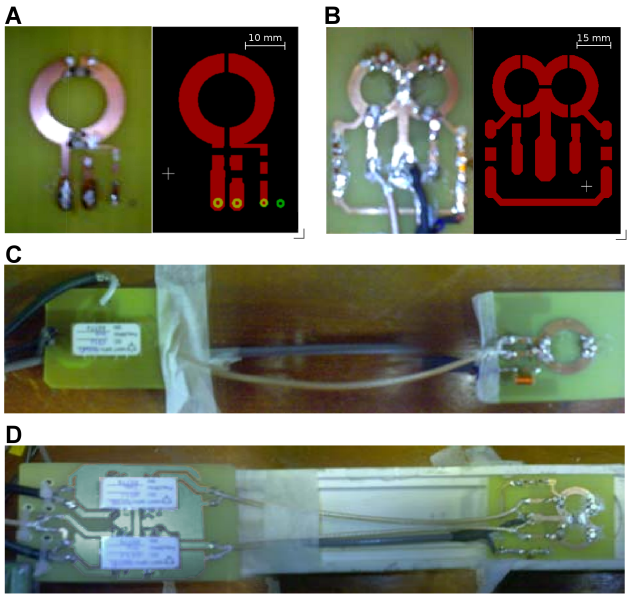

Fig. 1. **A**.Single loop device (SD) **B**. Two elements device (DD), using a shared capacitor for decoupling. **C**. Single loop device with pre-amplifier (SDWP) connected trough a $\frac{\lambda}{4}$ cable. **D**. Two elements device with pre-amplifier (DDWP), using a shared capacitor and connected trough a $\frac{\lambda}{4}$ cable.

per device. The five most centered slices in the volume of interest of each experiment are used to compute statistical comparisons (see **Table I**).

A. *Measures of receptors' performance and comparisons*

Measures of SNR, field stability and visual depth are done in the acquired images. The SNR is obtained in the time-domain as the ratio between the signal - high intensity pixels in FOV - and the standard deviation of the intensities in the background. The field stability is characterized by a filtered version of the horizontal profile, while visual depth is obtained from the vertical profiles, where amplitude and signal decay are separately analyzed. All measures are done in axial views. In order to assess the normality of the distribution, a Shapiro-Wilk test is run over the data. Then, T and Mann-Whitney U tests are used for statistical comparisons in normal and non-normal distributions, respectively. **Table I** summarizes the statistical approaches and lists the questions that we addressed with each test. Statistical significance is assessed using $\alpha = 0.05$. All the statistics mentioned above are computed with Python.

III. Results

This section presents the results of applying the measurements described in Subsection II-A. Color coding and labeling are provided in all figures of this section for easy association between the result and the device being tested.

A. *Gathering SNR data*

For each device, the SNR was measured by taking as signal a disk in the high intensity region at the center of the image and, as noise, the standard deviation of intensities in the rest of the FOV. See **Fig. 2**.

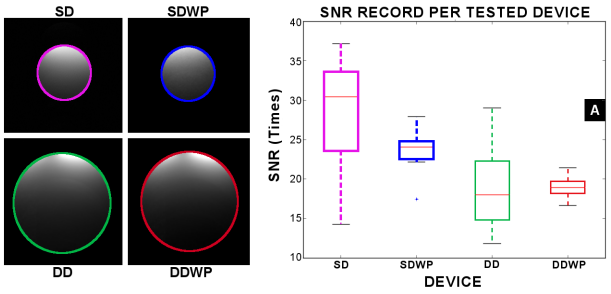

Fig. 2. Panel A. Single loop devices exhibit a higher image quality as measured by the SNR, nevertheless it is in this group where the pre-amplifier generates the highest gap in quality when comparing with its counterpart (SDWP). Remarkably, in both single and double device groups, the use of the pre-amplifier reduces the noise dispersion. In the double loop devices, the pre-amplifier does not modify the SNR.

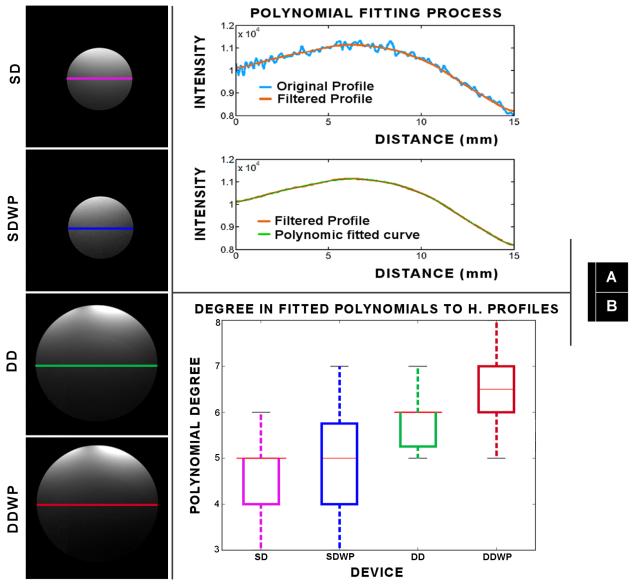

Fig. 3. Panel A. Summary of the procedure for the horizontal profiles. Panel B. Distribution in tortuosity of the horizontal profiles in each device, measured as the degree of the first polynomial adjusted at 0.995 index of correlation.

B. *Gathering Horizontal profile data*

A Gaussian filter is applied to the original profile with the aim of recovering its low frequency component, which is in turn, a measure of the field stability. The cutoff frequency is automatically extracted from the properties of the given profile by truncating its Fourier spectrum at 90% of the spectral energy content. Posteriorly, a homemade program iteratively looks for a polynomial that fits the filtered signal. See **Fig. 3**.

C. *Gathering decay and amplitude data*

The vertical profile provides two types of features, the amplitude and signal decay. These features can be separated for this specific analysis since the peak amplitude of the signal depends solely of construction specifications while the signal decay is a function of the recruited spins. Considering that the phantom contains the same solution for all tested

TABLE I

QUESTIONS ADDRESSED AND STATISTICAL TESTS PERFORMED

Factor	Test	Comparisons	Addressed question
SNR	T-test	(SD-SDWP)	Is the quality of the images affected by addition of the pre-amplifier?
SNR	T-test	(DD-DDWP)	Is the quality of the images affected by the addition of the pre-amplifier when the shared capacitor decoupling strategy is in place?
Horizontal	MWU	(SD-SDWP)	Is the field homogeneity affected by the pre-amplifier?
Horizontal	MWU	(DD-DDWP)	Is the field homogeneity affected by the pre-amplifier if other MI avoiding strategy is being used?
Amplitude	MWU	(SD-SDWP)	Is the amplitude of the acquisitions affected by the use of the pre-amplifier?
Amplitude	MWU	(DD-DDWP)	Is the amplitude of the acquisitions affected by the use of the pre-amplifier when the shared capacitor avoiding strategy is in place?
Decay	MWU	(SD-SDWP)	Is the use of the pre-amplifier affecting the visual depth?
Decay	MWU	(DD-DDWP)	Is the visual depth affected when the pre-amplifier is implemented with the shared capacitor MI avoiding strategy?
Decay	MWU	(SD-DD)	Is the visual depth of the coils increased when the inner diameter of the device decreases?
Decay	MWU	(SDWP-DDWP)	Is visual decay affected when two MI avoiding strategies are implemented together?

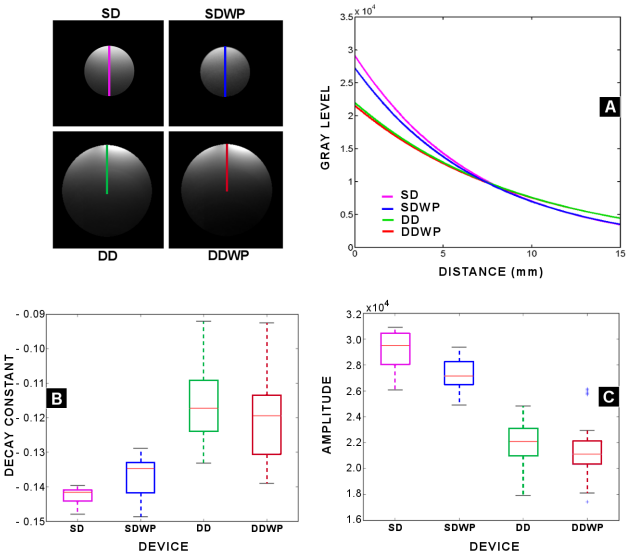

Fig. 4. Panel A shows the decay while penetrating the phantom in all devices. Panels B and C show the data distribution in decay and amplitude respectively for each tested device.

devices, the signal decay can be compared among all these devices, but an amplitude comparison will only be fair and conclusive if it is done intra-group. See **Fig. 4**.

IV. DISCUSSION

Our hypothesis was that DD devices behave similarly to SD devices when MI is diminished or avoided, and this claim is supported in those experiments where no statistical differences are found. Hence, we focus the discussion on those experiments that resulted in statistical differences, and on their practical implications. In what follows, the reader should refer to the significant entries marked with * in **Table II**, and follow the discussion according to their order in the Table.

A significant difference ($U = 247.5$, $Z = 3.22$, $p = 0.001$) is found between DD ($\overline{x} = 5.6 \pm 0.85$) and DDWP ($\overline{x} = 6.5 \pm 0.97$). The mean rank of DD was 32.25 and that of DDWP was 23.75. This results has low practical impact since the horizontal dynamics can be controlled by software reconstruction. In this case, we used a geometrically driven algorithm to merge the two channels, but customized setups can be implemented to optimize the smoothness of the boundary [2]. Nevertheless, the high degree of the fitted polynomials, even in the single loop devices, suggest a lack of uniformity in the cooper deposition of our devices. This is can be seen in **Fig. 3**, which belongs to the SD device. A perfectly build coil within a flat B_0 field should have a profile that can be modeled with a two-degree polynomial.

In the amplitude analysis, there was a significant difference between SD ($\overline{x} = 29096.36 \pm 1586.54$) and SDWP ($\overline{x} = 27222 \pm 1315.57$) ($U = 731.0$, $Z = -14.15$, $p = 0.0013$). The mean rank of SD was 21.13 and the mean rank of SDWP was 39.87, suggesting that the use of the pre-amplifier negatively affected the reading capabilities of the device. However, there are no practical implications to this finding, since it affects the single loop devices where the pre-amplifier does not introduce any added value. The pre-amplifier was connected to a single loop device with the purpose of creating a fair counterpart to compare the outcomes of the DDWP device. More importantly, the pre-amplifier in DD devices does not result in statistical differences, a fact of high relevance towards applicability.

In the decay analysis, there is a significant difference ($U = 193.50$, $Z = -3.79$, $p < 0.001$) between SD ($\overline{x} = -14.24 \pm 0.002$) and SDWP ($\overline{x} = -0.1366 \pm 0.005$). The mean rank of SD decay is 21.95 and the mean rank of SDWP decay is 39.05. There is no significant difference ($U = 533.0$, $Z = 1.23$, $p = 0.22$) between DD ($\overline{x} = -0.115 \pm 0.010$) and DDWP ($\overline{x} = -0.119 \pm 0.012$). The mean rank of DD decay is 33.27 and that of DDWP decay is 27.73. These results imply that visual depth is affected by the pre-amplifier in the group of devices that are not affected by the MI. In contrast, the pre-amplifiers do not have significant influence on the signal in DD devices,

TABLE II

RESULTS OF STATISTICAL TESTS. * EXPERIMENTS WHERE STATISTICAL DIFFERENCES ARE FOUND

Factor	Test	Comparisons	Average $\overline{x}\pm$ Standard deviation	p-value	Statistic values
SNR	T-test	(SD-SDWP)	(28.5 ± 7.95),(23.4 ± 3.48)	0.16	t=1.47 df=14
SNR	T-test	(DD-DDWP)	(19.0 ± 6.35),(18.9 ± 1.64)	0.97	t=0.03 df=9
Field stability	MWU	(SD-SDWP)	(4.4 ± 0.86),(4.7 ± 1.33)	0.41	U= 396.5, Z=0.83
Field stability	MWU	(DD-DDWP)	(5.6 ± 0.85),(6.5 ± 0.97)	0.001*	U=247.5, Z=3.22
Amplitude	MWU	(SD-SDWP)	(29096.3 ± 1586.54),(27222.0 ± 1315.57)	0.001*	U=731.0, Z=-4.15
Amplitude	MWU	(DD-DDWP)	(21971.4 ± 1665.32),(21526.8 ± 2375.99)	0.142	U=550.0, Z=-1.48
Decay	MWU	(SD-SDWP)	(-14.24 ± 0.002),(-0.12 ± 0.005)	0.0002*	U=193.5, Z=-3.79
Decay	MWU	(DD-DDWP)	(-0.11 ± 0.010),(-0.12 ± 0.012)	0.224	U=533.0, Z=1.23
Decay	MWU	(SD-DD)	(-0.142 ± 0.002),(-0.115 ± 0.010)	0.001*	U=900.0, Z=6.65
Decay	MWU	(SDWP-DDWP)	(-0.136 ± 0.005),(-0.119 ± 0.012)	0.001*	U=109.5, Z=5.03

where MI exists.

There was also a significant difference ($U = 900.0$, $Z = 6.65$ $p < 0.001$) between SD ($\overline{x} = -0.142 \pm 0.002$) and DD ($\overline{x} = -0.115 \pm 0.010$). The mean rank of SD decay was 45.50 and the mean rank of DD decay was 15.50. The reduction of the diameter in the coils improves the reading capabilities of these devices. There was a significant difference between SDWP ($\overline{x} = -0.136 \pm 0.005$) and DDWP ($\overline{x} = -0.119 \pm 0.012$); ($U = 109.5$, $Z = 5.03$, $p < 0.001$). The mean rank of SDWP decay was 41.85 and the mean rank of DDWP decay was 19.15, which suggest that both strategies can be used together without affecting the quality of the images.

V. CONCLUSIONS

We demonstrated that MI avoiding strategies can be used together without significantly affecting the signal quality. This fact opens the possibility of creating compounded devices that allows for flexible receptors. Moreover, several parallel imaging techniques such as Simultaneous Acquisition of Spatial Harmonics (SMASH) [14], Sensitivity Encoding (SENSE) [9], Generalized Auto Calibrating Partially Parallel Acquisitions (GRAPPA) [6], [10] and their improvements or variations [3], could be implemented to speed up acquisitions. The benefits of being more time effective in MRI are countless. For instance, the saved time could be used to improve the image quality in animal frameworks, where animal welfare is of high relevance. It could also have implications in human frameworks where shorter acquisition times would make MRI specialized methods such as high angular resolution diffusion imaging (HARDI), functional MRI (fMRI) among others, suitable not only for research purposes but also for the clinics, broadening the set of assistant tools for physicians. In addition, by improving the image quality in the acquisition stage, all the actual post-processing methods will be more efficient.

REFERENCES

[1] R. M. Arnold. Transmission Line Impedance Matching Using the Smith Chart. *IEEE Transactions in Microwave Theory Technology*, 22(11):977–978, 1974.

[2] O. Beuf, F. Jaillon, and H. Saint-Jalmes. Small-animal MRI: Signal-to-noise ratio comparison at 7 and 1.5 T with multiple-animal acquisition strategies. *Magn Reson Mater Phy*, 19:202 – 208, 2006.

[3] M. Blaimer, F. Breuer, M. Mueller, R. M. Heidemann, M. A. Griswold, and P. M. Jakob. SMASH, SENSE, PILS, GRAPPA How to Choose the Optimal Method. *Magn Reson Imaging*, 15(4):1 – 10, 2004.

[4] Cadsoftusa. Eagle pcb software, 2008.

[5] D. Gareis, T. Wichmann, T. Lanz, G. Melkus, M. Horn, and P. M. Jakob. Mouse MRI using phased-array coils. *NMR Biomed.*, 20:326 – 334, 2007.

[6] M. A. Griswold, P. M. Jakob, R. M. Heidemann, M. Nittka, V. Jellus, J. Wang, B. Kiefer, and A. Haase. Generalized autocalibrating partially parallel acquisitions. GRAPPA. *Science*, 47:1202 – 1210, 2002.

[7] F. Hennel. Experiment Programming with ParaVision on BioSpec and PharmaScan Systems. pages 28–32, 2002.

[8] J. Lian and P.B. Roemer. Mri rf coil, September 8 1998. US Patent 5,804,969.

[9] K. P. Pruessmann, M. Weiger, M. B. Scheidegger, and P. Boesiger. SENSE: Sensitivity Encoding for Fast MRI. *Magnetic Resonance in Medicine*, 42(3030):952 – 962, 1999.

[10] P. Qu, G. X. Shen, C. Wang, B. Wu, and J. Yuan. Tailored utilization of acquired k-space points for GRAPPA reconstruction. *Journal of Magnetic Resonance*, 174:60 – 67, 2005.

[11] Arne Reykowski, Steven M. Wright, and Jay R. Porter. Design of Matching Networks for Low Noise Preamplifiers. *Magnetic Resonance in Medicine*, (33):848–852, 1995.

[12] P.B. Roemer, W.A. Endelstein, C.E. Hayes, S.P. Souza, and O.M. Mueller. The NMR Phased Array. *Magenetic Resonance In Medicine*, (16):192–225, 1990.

[13] K. Sahay and S. Pathak. *Basic Concepts Of Electrical Engineering*. New Age International, 2006.

[14] DK Sodickson and WJ Manning. Simultaneous acquisition of spatial harmonics (SMASH): fast imaging with radiofrequency coil arrays. *Magnetic Resonance in Medicine*, 38:591–603, 1997.